

Polymer Solar Cells with Diketopyrrolopyrrole Conjugated Polymers as the Electron Donor and Electron Acceptor

Weiwei Li, W. S. Christian Roelofs, Mathieu Turbiez, Martijn M. Wienk, and René A. J. Janssen*

Conjugated polymers based on the diketopyrrolopyrrole (DPP) unit are successfully applied in field-effect transistors (FETs)^[1,2] and in polymer solar cells as electron donor.^[3,4] Record high mobilities for holes up to $10 \text{ cm}^2 \text{ V}^{-1} \text{ s}^{-1}$ have been realized, partially as a result of the tendency of DPP polymers to crystallize.^[5] In bulk-heterojunction solar cells, power conversion efficiencies (PCEs) up to 8% with fullerene as electron acceptor have been achieved, exploiting the broad absorption of DPP polymers to the near infrared region.^[6] Interestingly, several DPP polymers also show excellent electron mobilities in FETs.^[7–11] Combined, these properties raise the question as to whether it is possible to create a bulk-heterojunction solar cell that uses DPP-based semiconducting polymers both as electron donor and as electron acceptor. Intrigued by this question, we designed and synthesized a new semiconducting DPP polymer and demonstrate its use as electron acceptor in polymer-polymer solar cells with a second DPP polymer as electron donor.

Polymer-polymer solar cells, in which conjugated polymers are used both as electron donor and electron acceptor, are attracting renewed attention.^[12–25] Polyera announced obtaining a power conversion efficiency (PCE) of 6.4% for proprietary materials.^[26] For known materials, the highest value published to date is PCE = 4.1%.^[14] These recent results give credence to the belief that polymer-polymer solar cells can close the gap to the best polymer-fullerene bulk-heterojunction solar cells that have reached PCEs = 9–10%.^[27–29]

The structural and electronic variation in electron-acceptor conjugated polymers is virtually infinite and offers much wider possibilities for varying the electronic structure and optical bandgap compared with fullerene derivatives. The energy levels, optical bandgap, crystallinity, and charge mobility, can all be adjusted toward improving the power conversion efficiencies. Numerous alternating electron push-pull copolymers have been explored as electron donor,^[30,31] but – despite the advantages mentioned above – conjugated polymers that can act as electron acceptor in efficient solar cells are rather underdeveloped.^[12] So far, only a few successful conjugated

electron-acceptor polymers are known. Among these are cyanopolyphenylenevinylenes,^[24,32] copolymers of benzothiadiazole and fluorene,^[21,22,33–36] and copolymers incorporating perylene-diiimide or naphthalenediimide acceptor units.^[14–20] Electron-acceptor polymers based on isoindigo^[37] or diketopyrrolopyrrole (DPP)^[38] have only given low PCEs (<1%) in polymer-polymer solar cells until now.

The primary design strategy for an electron-accepting conjugated polymer is to create a complementary energy level alignment with an electron-donating polymer, such that it provides enough driving force for exciton dissociation into free charges. The free energy for charge generation is determined by the difference between the exciton energy, or optical gap (E_g), and the energy of the charge transfer (CT) state at the interface (E_{CT}). These energies are related to the highest occupied molecular orbital (HOMO) and lowest unoccupied molecular orbital (LUMO) levels of the donor and the acceptor. It has been found experimentally that the offsets between the energies of the two HOMO and the two LUMO levels should both be ca. 0.35 eV or more to ensure charge transfer.^[39] Energy-level control can be achieved by incorporating suitable electron-donating or electron-deficient moieties in the conjugated backbone.^[30] Next to proper energy levels, a high electron mobility is needed for a successful acceptor polymer to ensure efficient electron transport to the electrode. It has been shown that trap-free electron transport can only be obtained in conjugated polymers with an electron affinity larger than ca. 3.6 eV.^[40] In addition, the electron mobility will be enhanced via interchain interactions and three-dimensional order. Enhanced crystallinity is also beneficial in creating efficient percolating pathways for hole and electron transport via microphase separation.^[41] Several publications have shown that it is possible to improve the microphase separation and the PCE by augmenting the processing solvent with a processing additive,^[17,41,42] which is a well-known method used for morphology control in polymer:fullerene solar cells.

Our design for an n-type DPP acceptor polymer starts from the copolymer of DPP and terthiophene (PDDP3T). As electron donor, PDDP3T affords a PCE of 7.4% in polymer solar cells when blended with [70]PCBM as the electron acceptor.^[6] Although PDDP3T has a relatively low LUMO level (–3.74 eV), its HOMO level (–5.30 eV) is not sufficiently deep to make it a successful electron acceptor in blends with most electron-donor conjugated polymers. To decrease the HOMO level, we replace thiophene by thiazole to form PDDP2TzT (Figure 1) in which the electronegative imine nitrogens (C=N–C) effectively lower the HOMO and LUMO energy levels.^[35,43,44] We find that PDDP2TzT has an electron mobility of $0.13 \text{ cm}^2 \text{ V}^{-1} \text{ s}^{-1}$ in a FET and can be used as electron acceptor in all-polymer

Dr. W. W. Li, W. S. C. Roelofs,
Dr. M. M. Wienk, Prof. R. A. J. Janssen
Molecular Materials and Nanosystems
Eindhoven University of Technology
P.O. Box 513, 5600, MB, Eindhoven, The Netherlands
E-mail: r.a.j.janssen@tue.nl

Dr. M. Turbiez
Organic Electronic Materials Basel
BASF Schweiz AG
Schwarzwaldallee 215, 4002, Basel, Switzerland



DOI: 10.1002/adma.201305910

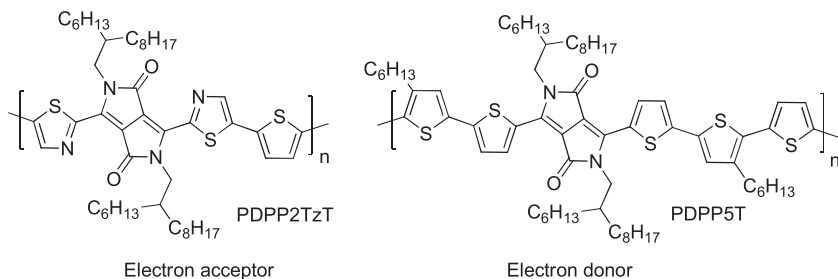


Figure 1. The newly designed PDPP2TzT electron-acceptor and PDPP5T electron-donor polymers used in this work.

solar cells with a PCE = 2.9% in combination with a second DPP-polymer (PDPP5T, Figure 1) as donor. The complementary electron donor and acceptor polymers differ only by the interchange of bithiophene and thiazole units along the polymer chain (Figure 1), demonstrating how relatively small changes in molecular structure can be used to modify electronic properties.

PDPP2TzT was synthesized from bis(bromothiazolyl)-DPP (DPP2TzBr) and bis(trimethylstannyl)thiophene via a Stille polymerization. The DPP2TzBr monomer was obtained via the procedure reported by Carsten et al.,^[44] using a modification as detailed in the Supporting Information. High-molecular-weight PDPP2TzT was obtained by performing the reaction in toluene/DMF (10:1 v/v) and using Pd₂(dba)₃/PPh₃ (1:4 mol/mol) as a catalyst. The molecular weight of PDPP2TzT ($M_n = 93.3 \text{ kg mol}^{-1}$, $M_w = 284.7 \text{ kg mol}^{-1}$, PDI = 3.05) was determined by gel-permeation chromatography (GPC) using a low concentration in *o*-dichlorobenzene (*o*-DCB) (0.06 mg mL⁻¹) at an elevated temperature (80 °C) to reduce aggregation (Supporting Information, Figure S1). A high molecular weight, as found for PDPP2TzT, is generally helpful for reaching a high performance in polymer solar cells.^[45,46]

In thin films PDPP2TzT exhibits an absorption in the near infrared region with an optical bandgap of $E_g = 1.44 \text{ eV}$ (Figure 2). The absorption in thin films is slightly red-shifted with respect to the absorption in chloroform solution (Supporting Information, Figure S2). Compared with PDPP3T, with $E_g = 1.30 \text{ eV}$, replacing of thiophene by thiazole widens the optical bandgap. The oxidation and reduction potentials of PDPP2TzT were determined by cyclic voltammetry in *o*-DCB solution (Supporting Information, Figure S3, Table S1).

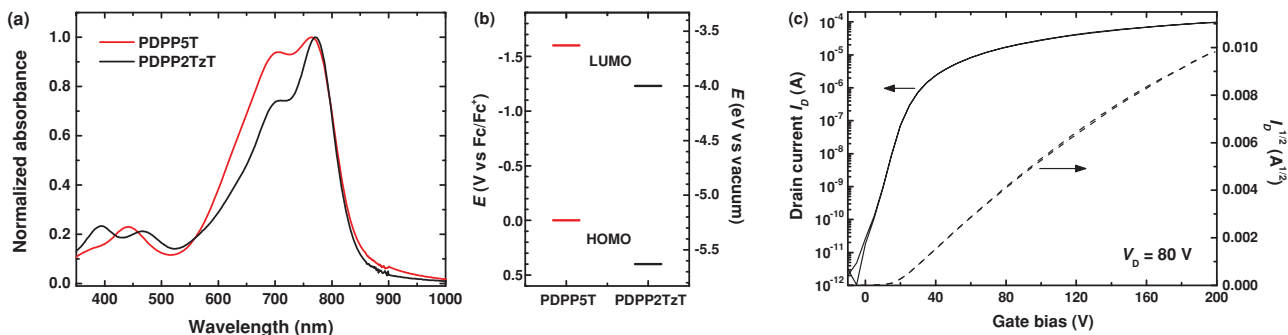


Figure 2. a) Absorption spectra of thin films of PDPP5T (red line) and PDPP2TzT (black line). b) Energy levels determined from cyclic voltammetry ($E(\text{Fc}/\text{Fc}^+) = -5.23 \text{ eV}$). c) Transfer characteristics of a bottom-contact top-gate field-effect transistor of PDPP2TzT. The applied drain bias V_D was 80 V.

PDPP2TzT has a low-lying HOMO level at -5.63 eV and a LUMO level at -4.00 eV . Both levels are lowered by about 0.3 eV compared with PDPP3T (HOMO at -5.30 eV and LUMO at -3.74 eV) as a consequence of replacing the two thiophenes by two thiazoles. The LUMO level of PDPP2TzT is close to that of [70]PCBM (LUMO at -4.16 eV , see Supporting Information).

The charge-carrier mobility of PDPP2TzT was studied in FETs with a bottom-contact top-gate configuration. Under these conditions, the electron mobility is $\mu_e = 0.13 \text{ cm}^2 \text{ V}^{-1} \text{ s}^{-1}$

(Figure 2c), comparable to $\mu_e = 0.2 \text{ cm}^2 \text{ V}^{-1} \text{ s}^{-1}$ reported for [60]PCBM in a similar configuration.^[47] The hole mobility for PDPP2TzT is relatively low ($\mu_h = 6 \times 10^{-3} \text{ cm}^2 \text{ V}^{-1} \text{ s}^{-1}$), which is different from other DPP-polymers with ambipolar behavior. This probably results from a limited hole injection due to the deep HOMO level of PDPP2TzT.

The low-lying energy levels, the high electron mobility, and the near-infrared absorption spectrum make PDPP2TzT a promising electron acceptor for polymer-polymer solar cells. We selected PDPP5T as the complementary donor because it has relatively high HOMO (-5.23 eV) and LUMO (-3.63 eV) levels (Figure 2b and Table S1, Supporting Information) that provide a large enough energy offset ($>0.35 \text{ eV}$) with the HOMO and LUMO of PDPP2TzT to enable efficient charge dissociation. The optical bandgap of PDPP5T is very similar to that of PDPP2TzT (Figure 2a). Additionally, PDPP5T has shown to be an excellent electron donor polymer when blended with [70]PCBM, giving a PCE of 6% (Supporting Information, Figure S4 and Table S2).

Polymer-polymer solar cells based on PDPP5T:PDPP2TzT blends were made in an inverted device configuration using transparent indium tin oxide (ITO)/ZnO and reflective MoO₃/Ag electrodes to collect electron and holes, respectively. The PDPP5T:PDPP2TzT photoactive layer was spin-coated from chloroform. Without the use of a processing additive, the performance is poor (PCE = 0.33%, Table 1 and Figure 3). The low fill factor (FF = 0.34) suggests significant bimolecular charge recombination, which would be expected for an intimately mixed PDPP5T:PDPP2TzT blend. When a small amount of 1,8-diiodooctane (DIO) was used as a high-boiling-point processing additive, the PCE improved to 0.79%. Addition of

Table 1. Characteristics of PDPP5T:PDPP2Tz (1:0.8) solar cells spin coated from chloroform solution with different processing additives.

Solvent	$J_{sc}^a)$ [mA cm ⁻²]	V_{oc} [V]	FF	PCE ^{a)} [%]
CHCl ₃ ^{b)}	1.2	0.79	0.34	0.33
CHCl ₃ :DIO 2.5% ^{b)}	2.4	0.81	0.41	0.79
CHCl ₃ :1-DB 5% ^{b)}	3.3	0.83	0.42	1.2
CHCl ₃ : <i>o</i> -DCB 20% ^{b)}	5.0	0.80	0.47	1.9
CHCl ₃ :1-CN 7.5% ^{b)}	6.9	0.81	0.51	2.9
CHCl ₃ :1-CN 7.5% ^{c)}	5.3	0.79	0.47	2.0

^{a)} J_{sc} was calculated by integrating the EQE spectrum with the AM1.5G spectrum;

^{b)}Device configuration with ITO/ZnO and MoO₃/Ag electrodes; ^{c)}Device configuration with ITO/PEDOT:PSS and LiF/Al electrodes.

aromatic processing additives such as 1-dodecylbenzene (1-DB) and *o*-DCB further enhance the PCE to 1.2% and 1.9% (Supporting Information, Figure S5). The highest PCE of 2.9% was obtained using 1-chloronaphthalene (1-CN) (7.5 vol%), a PDPP5T:PDPP2TzT ratio of 1:0.8 (w/w), and a layer thickness of 80 nm. The DPP polymers are not sufficiently soluble in

aromatic solvents to use these as a the primary solvent for layer deposition.^[3]

The improved performance obtained with the processing additives is a result of an increase in short-circuit current density from $J_{sc} = 1.2$ to 6.9 mA cm⁻² and a concomitant increase in fill factor from FF = 0.34 to 0.51. The open-circuit voltage remains constant at $V_{oc} \approx 0.80$ V. The enhanced J_{sc} is also reflected in the improved external quantum efficiency (EQE), which increases from 0.05 to 0.29 at 760 nm (Figure 3b). The cells exhibit a broad spectral response from 350 nm to 850 nm. The V_{oc} of 0.81 V of the optimized cell is significantly higher than the V_{oc} of 0.57 V of PDPP5T:[70]PCBM cells. As a consequence, the photon energy loss, defined as $E_g - eV_{oc}$, is reduced to 0.63 eV, which is close to the optimized energy loss for exciton dissociation.^[48]

The morphology and phase separation of the photoactive layers was investigated with atomic force microscopy (AFM) (Figure 4). Blends spin-coated from pure chloroform have a smooth surface with a root-mean-square (RMS) roughness of $R_q = 1.01$ nm, but show small fibrillar structures in the phase image (Figure 4d). The smooth surface suggests that a large phase separation is absent, consistent with the very low FF. DPP polymers have a strong tendency to form crystalline fibrils, which are also found in PDPP5T:[70]PCBM and PDPP2TzT:[70]PCBM blend films (TEM image, Supporting Information, Figure S6 and S7). We speculate that the fibrils in the PDPP5T:PDPP2TzT films from chloroform contain both PDPP5T and PDPP2TzT, resulting in charge recombination and hence low J_{sc} and FF. Enhanced phase separation in the blend films is observed using DIO or 1-CN as an additive. Larger domains and more surface corrugation are seen in the AFM images, and the roughness increased to $R_q = 2.69$ and 3.40 nm. Even though the real reason is unclear, we assume that the solubility difference of PDPP5T and PDPP2TzT in DIO and 1-CN creates the change in phase separation.

PDPP2Tz functions as an acceptor with a variety of donors, provided that the energy level offsets are correct. With P3HT as donor it is possible to make polymer-polymer solar with PCE = 0.6% ($J_{sc} = 1.7$ mA cm⁻², $V_{oc} = 0.66$ V, FF = 0.54) when using a 1:1 weight ratio and spin coating from chloroform containing 3 vol% 1-CN (Supporting Information, Figures S8, S9)

In our experiments with PDPP5T:PDPP2TzT cells, we observed that the inverted device configuration with ITO/ZnO and MoO₃/Ag electrodes gives a PCE = 2.9%, which is significantly higher than the PCE = 2.0% for a regular device configuration with ITO/poly(3,4-ethylenedioxythiophene) poly(styrenesulfonate) (PEDOT:PSS) bottom and LiF/Al top electrodes (Table 1 and Supporting Information, Figure S10). The decrease for the regular device mainly results from a drop in J_{sc} and is also evident in the EQE (Figure 5a). The active layers for both device configurations were spin coated from the same solution (chloroform with 7.5% 1-CN) and with AFM there is no observable difference in the microphase separation (Supporting Information, Figure S11). To explain the difference, we determined the wavelength-dependent extinction (k) and refractive index (n) (Supporting Information, Figure S12) and calculated the absorption profile, the relative fraction of absorbed photons, and the internal quantum efficiency (IQE) using the transfer-matrix formalism, taking into account the

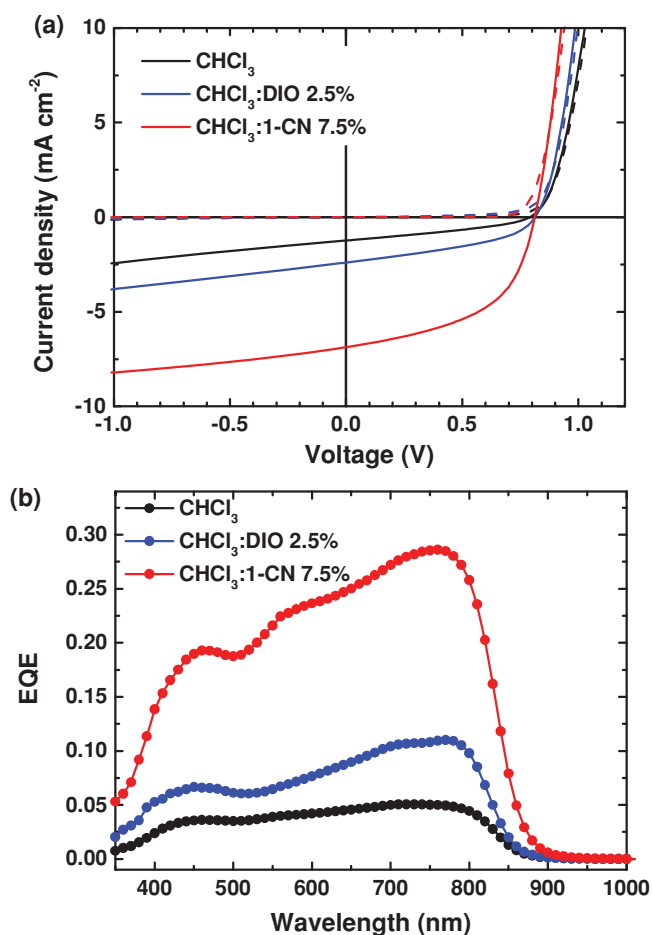


Figure 3. a) J - V characteristics in the dark (dashed lines) and under white-light illumination (solid lines) of optimized inverted solar cells of PDPP5T:PDPP2TzT (1:0.8 w/w), spin-coated from chloroform solution without or with additive. b) EQE of the same devices.

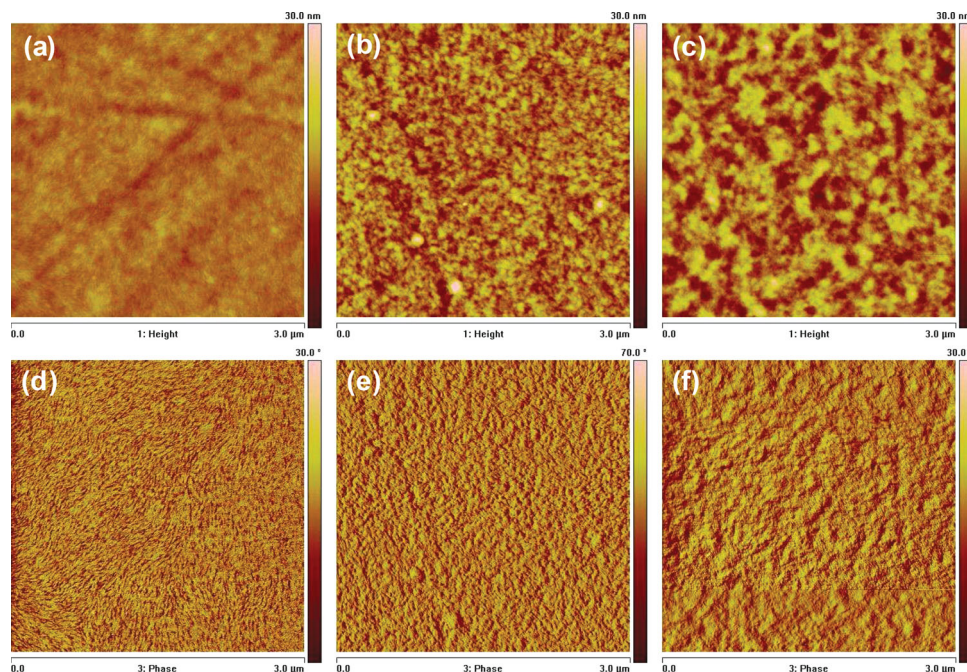


Figure 4. AFM height images ($3 \mu\text{m} \times 3 \mu\text{m}$, vertical scale 30 nm) of optimized PDPP5T:PDPP2TzT blends spin-coated from: a) chloroform, b) chloroform containing 2.5% DIO, and c) chloroform containing 7.5 vol.% 1-CN. The root-mean-square (RMS) roughnesses are 1.01 nm, 2.69 nm and 3.40 nm from (a) to (c). d–f) Phase images ($3 \mu\text{m} \times 3 \mu\text{m}$, vertical scale 30°) corresponding to the height images (a) to (c).

optical constants of all layers in the cells (Figure 5b–d). The results reveal that the PDPP5T:PDPP2TzT layer absorbs more photons in an inverted configuration than in the regular configuration. This is mainly due to a higher photon absorption by PEDOT:PSS and Al compared with ZnO and MoO₃/Ag (Figure 5b and Supporting Information, Figure S13).

There is, however, another process that contributes to the difference and this relates to the light-absorption profile. In the inverted configuration ca. 75% of the photons are absorbed in the first 40 nm of the 80 nm thick layer. If electron transport is limiting, this is beneficial because ca. 75% electrons have to migrate less than half of the layer thickness (≤ 40 nm) to reach the electrode. In contrast, for the regular configuration only ca. 35% of the electrons are generated within 40 nm of the electron collecting LiF/Al contact. Hence, most of the electrons (ca. 65%) have to travel more than half of the layer thickness (≥ 40 nm) and consequently have a higher chance of recombining. Support for this explanation is seen in the IQE which is higher for the inverted configuration than for the regular configuration over almost the entire wavelength region (Figure 5d).

In conclusion, a new *n*-type acceptor polymer PDPP2TzT based on diketopyrrolopyrrole has been designed and synthesized. The polymer features low-lying HOMO and LUMO energy levels, high electron mobility, and a broad absorption up to 850 nm. When the new acceptor was blended with PDPP5T as electron-donor polymer, a PCE of 2.9% was obtained after optimizing the solvent composition with a processing additive to adjust the phase separation. A higher PCE was found in inverted devices than in regular devices, which is due to enhanced photon absorption and charge collection in the inverted device. From a molecular design perspective we note that the donor and acceptor polymer are very much alike. The

donor and acceptor DPP polymers merely differ by the simple interchange of electron-rich bithiophene units by electron-deficient thiazole units along the chain. The results show that DPP polymers form an interesting new class of acceptor *n*-type polymers, which approach the performance of perylene diimide or naphthalene diimide acceptor copolymers.^[14–20]

Experimental Section

Inverted configuration photovoltaic devices were made by spin-coating a ZnO sol-gel^[49] at 4000 rpm for 60 s onto precleaned, patterned ITO substrates (14Ω per square) (Naranjo Substrates). A 40 nm-thick ZnO layer was formed and baked at 150°C for 5 min in air. The photoactive layer was deposited by spin-coating a chloroform solution containing the PDPP5T and PDPP2TzT with different ratios and the appropriate amounts of additive in air. MoO₃ (10 nm) and Ag (100 nm) were deposited by vacuum evaporation at ca. 2×10^{-7} mbar as the back electrode. For polymer–polymer solar cells in the regular configuration and for polymer solar cells with PDPP5T or PDPP2TzT as donor and [70]PCBM as acceptor, PEDOT:PSS (Clevios P, VP Al 4083) was spin-coated onto precleaned, patterned ITO substrates (14Ω per square) (Naranjo Substrates) and then annealed at 120°C for 10 min in N₂ filled glovebox. The photoactive layers were deposited by spin-coating a chloroform solution containing the donor and acceptor in the proper ratio and the appropriate amount of processing additive. LiF (1 nm) and Al (100 nm) were deposited by vacuum evaporation at ca. 2×10^{-7} mbar as the back electrode.

The active area of the cells was 0.09 or 0.16 cm² and no size dependence was found between these two dimensions. *J*–*V* characteristics were measured under ca. 100 mW cm^{-2} white light from a tungsten-halogen lamp filtered by a Schott GG385 UV filter and a Hoya LB 120 daylight filter, using a Keithley 2400 source meter. Short-circuit currents under AM1.5G conditions were estimated from the spectral response and convolution with the solar spectrum. The spectral response was measured under simulated 1 sun operation conditions

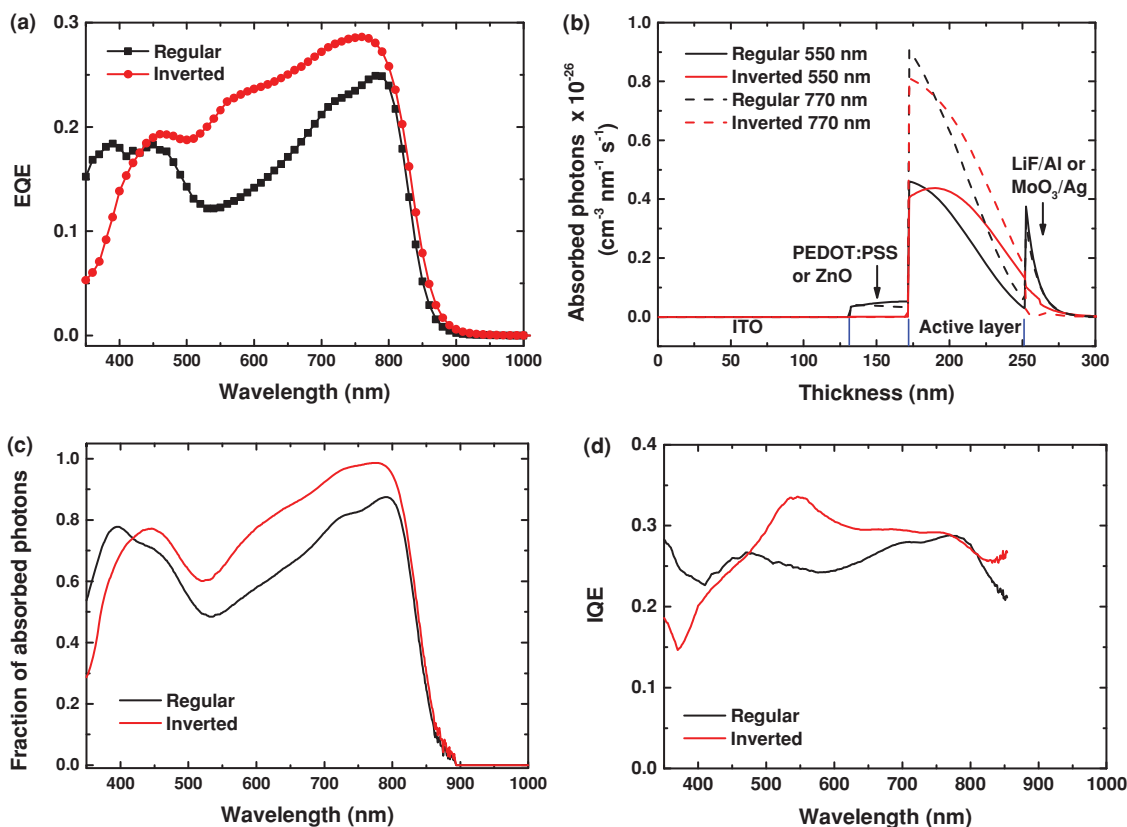


Figure 5. Comparison of regular and inverted device configuration. a) EQE. b) The simulated number of absorbed photons at 550 and 770 nm in regular or inverted devices (from glass side). The thickness of active layer is 80 nm. c) Fraction of absorbed photons. d) IQE related to wavelength for PDPP5T:PDPP2TzT (1:0.8) layers (80 nm). The averaged IQEs were 0.26 and 0.29 for the regular and inverted devices.

using bias light from a 532 nm solid state laser (Edmund Optics). Light from a 50 W tungsten halogen lamp (Osram64610) was used as probe light and modulated with a mechanical chopper before passing the monochromator (Oriel, Cornerstone 130) to select the wavelength. The response was recorded as the voltage over a 50 Ω resistance, using a lock-in amplifier (Stanford Research Systems SR 830). A calibrated Si cell was used as reference. The device was kept behind a quartz window in a nitrogen filled container. The thickness of the active layers in the photovoltaic devices was measured on a Veeco Dektak 150 profilometer.

Field-effect transistors were prepared in a bottom-contact top-gate configuration on a glass substrate. Source and drain contacts were defined by evaporating a 2 nm Cr adhesive layer and a 50 nm gold layer through a shadow mask. Subsequently the polymer was applied by spin-coating from a hot chloroform solution in an oxygen and water-free atmosphere. The polymer film was annealed at 200 $^{\circ}\text{C}$ for 20 min. Next, a 850 nm Cytop layer was spin-coated as gate dielectric and annealed at 140 $^{\circ}\text{C}$ for 20 min. The top-gate electrode was applied by evaporating Au (50 nm) through a shadow mask. The length and the width of the transistor channel were 30 μm and 1000 μm , respectively. The transistors were electrically characterized under high vacuum conditions with a Keithley 2400 measuring unit. The whole device was thermally annealed at 200 $^{\circ}\text{C}$ for 16 h in high vacuum before measuring to remove any traces of water.

AFM images were taken on a Veeco MultiMode AFM connected to a Nanoscope III controller operating in tapping mode using PPPNCH-50 probes (Nanosensors).

The IQE was determined by optical modeling of the entire layer stack using the wavelength dependent refractive index (n) and extinction coefficient (k).^[50] Calculations of the optical electric field were performed with Setfos 3 (Fluxim AG, Switzerland). The averaged IQE was determined by convolution of the solar spectrum with the EQE of the solar cell and the absorbed photon flux.

Supporting Information

Supporting Information is available from the Wiley Online Library or from the author.

Acknowledgements

The authors thank Alice Furlan and Hans van Franeker for TEM measurements and Ralf Bovee for GPC analysis. The work was performed in the framework of the Largecells project that received funding from the European Commission's Seventh Framework Programme (Grant Agreement No. 261936). The research forms part of the Solliance OPV programme and has received funding from the Ministry of Education, Culture and Science (Gravity program 024.001.035).

Received: December 1, 2013

Revised: January 1, 2014

Published online: March 26, 2014

- [1] L. Bürgi, M. Turbiez, R. Pfeiffer, F. Bienewald, H.-J. Kirner, C. Winnewisser, *Adv. Mater.* **2008**, *20*, 2217.
- [2] For a review see: C. B. Nielsen, M. Turbiez, I. McCulloch, *Adv. Mater.* **2013**, *25*, 1859.
- [3] M. M. Wienk, M. Turbiez, J. Gilot, R. A. J. Janssen, *Adv. Mater.* **2008**, *20*, 2556.
- [4] For reviews see: a) Y. Li, P. Sonar, L. Murphy, W. Hong, *Energy Environ. Sci.* **2013**, *6*, 1684; b) S. Qu, H. Tian, *Chem. Commun.* **2012**, *48*, 3039.

- [5] I. Kang, H.-J. Yun, D. S. Chung, S.-K. Kwon, Y.-H. Kim, *J. Am. Chem. Soc.* **2013**, *135*, 14896.
- [6] K. H. Hendriks, G. H. L. Heintges, V. S. Gevaerts, M. M. Wienk, R. A. J. Janssen, *Angew. Chem., Int. Ed.* **2013**, *52*, 8341.
- [7] J. C. Bijleveld, A. P. Zoombelt, S. G. J. Mathijssen, M. M. Wienk, M. Turbiez, D. M. de Leeuw, R. A. J. Janssen, *J. Am. Chem. Soc.* **2009**, *131*, 16616.
- [8] J. C. Bijleveld, V. S. Gevaerts, D. Di Nuzzo, M. Turbiez, S. G. J. Mathijssen, D. M. de Leeuw, M. M. Wienk, R. A. J. Janssen, *Adv. Mater.* **2010**, *22*, E242.
- [9] J. D. Yuen, J. Fan, J. Seifert, B. Lim, R. Hufschmid, A. J. Heeger, F. Wudl, *J. Am. Chem. Soc.* **2011**, *133*, 20799.
- [10] Z. Chen, M. J. Lee, R. Shahid Ashraf, Y. Gu, S. Albert-Seifried, M. Meedom Nielsen, B. Schroeder, T. D. Anthopoulos, M. Heeney, I. McCulloch, H. Sirringhaus, *Adv. Mater.* **2012**, *24*, 647.
- [11] W. W. Li, K. H. Hendriks, W. S. C. Roelofs, Y. Kim, M. M. Wienk, R. A. J. Janssen, *Adv. Mater.* **2013**, *25*, 3182.
- [12] A. Facchetti, *Mater Today* **2013**, *16*, 123.
- [13] R. McNeill, N. C. Greenham, *Adv. Mater.* **2009**, *21*, 3840.
- [14] D. Mori, H. Bente, I. Okada, H. Ohkita, S. Ito, *Adv. Energy Mater.* **2013**, DOI: 10.1002/aenm.201301006.
- [15] E. Zhou, J. Cong, K. Hashimoto, K. Tajima, *Adv. Mater.* **2013**, *25*, 6991.
- [16] T. Earmme, Y.-J. Hwang, N. M. Murari, S. Subramaniyan, S. A. Jenekhe, *J. Am. Chem. Soc.* **2013**, *135*, 14960.
- [17] N. Zhou, H. Lin, S. J. Lou, X. Yu, P. Guo, E. F. Manley, S. Loser, P. Hartnett, H. Huang, M. R. Wasielewski, L. X. Chen, R. P. H. Chang, A. Facchetti, T. J. Marks, *Adv. Energy Mater.* **2013**, DOI: 10.1002/aenm.201300785.
- [18] P. Cheng, L. Ye, X. Zhao, J. Hou, Y. Li, X. Zhan, *Energy Environ. Sci.* **2013**, DOI: 10.1039/c3ee43041c.
- [19] E. Zhou, J. Cong, Q. Wei, K. Tajima, C. Yang, K. Hashimoto, *Angew. Chem., Int. Ed.* **2011**, *50*, 2799.
- [20] X. Zhan, Z. A. Tan, B. Domercq, Z. An, X. Zhang, S. Barlow, Y. Li, D. Zhu, B. Kippelen, S. R. Marder, *J. Am. Chem. Soc.* **2007**, *129*, 7246.
- [21] D. Mori, H. Bente, H. Ohkita, S. Ito, K. Miyake, *ACS Appl. Mater. Interfaces* **2012**, *4*, 3325.
- [22] X. He, F. Gao, G. Tu, D. Hasko, S. Hüttner, U. Steiner, N. C. Greenham, R. H. Friend, W. T. S. Huck, *Nano. Lett.* **2010**, *10*, 1302.
- [23] C. R. McNeill, A. Abrusci, I. Hwang, M. A. Ruderer, P. Müller-Buschbaum, N. C. Greenham, *Adv. Funct. Mater.* **2009**, *19*, 3103.
- [24] T. Kietzke, H.-H. Hörhold, D. Neher, *Chem. Mater.* **2005**, *17*, 6532.
- [25] S. Fabiano, S. Himmelberger, M. Drees, Z. Chen, R. M. Altamimi, A. Salleo, M. A. Loi, A. Facchetti, *Adv. Energy Mater.* **2013**, DOI: 10.1002/aenm.201301409.
- [26] Released by Polyera in **2013**, <http://www.polyera.com/newsflash/polyera-achieves-6-4-all-polymer-organic-solar-cells>, accessed: February 2014.
- [27] J. You, L. Dou, K. Yoshimura, T. Kato, K. Ohya, T. Moriarty, K. Emery, C.-C. Chen, J. Gao, G. Li, Y. Yang, *Nat. Commun.* **2013**, *4*, 1446.
- [28] Z. C. He, C. M. Zhong, S. J. Su, M. Xu, H. B. Wu, Y. Cao, *Nat. Photonics* **2012**, *6*, 591.
- [29] W. W. Li, A. Furlan, K. H. Hendriks, M. M. Wienk, R. A. J. Janssen, *J. Am. Chem. Soc.* **2013**, *135*, 5529.
- [30] Y. J. Cheng, S. H. Yang, C. S. Hsu, *Chem. Rev.* **2009**, *109*, 5868.
- [31] L. Dou, J. You, Z. Hong, Z. Xu, G. Li, R. A. Street, Y. Yang, *Adv. Mater.* **2013**, *25*, 6642.
- [32] S. A. Jenekhe, S. Yi, *Appl. Phys. Lett.* **2000**, *77*, 2635.
- [33] D. Mori, H. Bente, J. Kosaka, H. Ohkita, S. Ito, K. Miyake, *ACS Appl. Mater. Interfaces* **2011**, *3*, 2924.
- [34] C. Arias, J. D. MacKenzie, R. Stevenson, J. J. M. Halls, M. Inbasekaran, E. P. Woo, D. Richards, R. H. Friend, *Macromolecules* **2001**, *34*, 6005.
- [35] Y. Cao, T. Lei, J. Yuan, J.-Y. Wang, J. Pei, *Polym. Chem.* **2013**, *4*, 5228.
- [36] Y. Zhou, Q. Yan, Y.-Q. Zheng, J.-Y. Wang, D. Zhao, J. Pei, *J. Mater. Chem. A* **2013**, *1*, 6609.
- [37] R. Stalder, J. Mei, J. Subbiah, C. Grand, L. A. Estrada, F. So, J. R. Reynolds, *Macromolecules* **2011**, *44*, 6303.
- [38] M.-F. Falzon, A. P. Zoombelt, M. M. Wienk, R. A. J. Janssen, *Phys. Chem. Chem. Phys.* **2011**, *13*, 8931.
- [39] M. C. Scharber, D. Mühlbacher, M. Koppe, P. Denk, C. Waldauf, A. J. Heeger, C. J. Brabec, *Adv. Mater.* **2006**, *18*, 789.
- [40] H. T. Nicolai, M. Kuik, G. A. H. Wetzelaer, B. de Boer, C. Campbell, C. Risko, J. L. Brédas, P. W. M. Blom, *Nat. Mater.* **2012**, *11*, 828.
- [41] M. Schubert, D. Dolfen, J. Frisch, S. Roland, R. Steyrluthner, B. Stiller, Z. Chen, U. Scherf, N. Koch, A. Facchetti, D. Neher, *Adv. Energy Mater.* **2012**, *2*, 369.
- [42] C. R. McNeill, *Energy Environ. Sci.* **2012**, *5*, 5653.
- [43] Y. Lin, H. Fan, Y. Li, X. Zhan, *Adv. Mater.* **2012**, *24*, 3087.
- [44] B. Carsten, J. M. Szarko, L. Lu, H. J. Son, F. He, Y. Y. Botros, L. X. Chen, L. Yu, *Macromolecules* **2012**, *45*, 6390.
- [45] R. C. Coffin, J. Peet, J. Rogers, G. C. Bazan, *Nat. Chem.* **2009**, *1*, 657.
- [46] S. Wakim, S. Beaupré, N. Blouin, B.-R. Aich, S. Rodman, R. Gaudiana, Y. Tao, M. Leclerc, *J. Mater. Chem.* **2009**, *19*, 5351.
- [47] T. B. Singh, N. Marjanovic, P. Stadler, M. Auinger, G. J. Matt, S. Günes, N. S. Sariciftci, R. Schwödiauer, S. Bauer, *J. Appl. Phys.* **2005**, *97*, 083714.
- [48] D. Veldman, O. Ipek, S. C. J. Meskers, J. Sweelssen, M. M. Koetse, S. C. Veenstra, J. M. Kroon, S. S. van Bavel, J. Loos, R. A. J. Janssen, *J. Am. Chem. Soc.* **2008**, *130*, 7721.
- [49] Y. Sun, J. H. Seo, C. J. Takacs, J. Seifert, A. J. Heeger, *Adv. Mater.* **2011**, *23*, 1679.
- [50] J. Gilot, M. M. Wienk, R. A. J. Janssen, *Adv. Mater.* **2010**, *22*, E67.